FEBS Letters 582 (2008) 3479–3483

Identification of amino acid residues important for the phosphomannose isomerase activity of PslB in *Pseudomonas aeruginosa* PAO1

Hui-Ju Lee[a], Hwan-You Chang[b], Nandinin Venkatesan[b], Hwei-Ling Peng[a,*]

[a] *College of Biological Science and Technology, National Chiao Tung University, 75 Po Ai Street, Hsin Chu, Taiwan*
[b] *Institute of Molecular Medicine, National Tsing Hua University, Hsin Chu 30010, Taiwan*

Received 2 July 2008; revised 9 September 2008; accepted 9 September 2008

Available online 16 September 2008

Edited by Stuart Ferguson

Abstract Phosphomannose isomerase (PMI) plays a pivotal role in biosynthesis of GDP-mannose, an important precursor of many polysaccharides. We demonstrate in this study that *Pseudomonas aeruginosa pslB* encodes a protein with GDP-mannose pyrophosphorylase/PMI dual activities. The PMI activity is Co^{2+}-dependent and could be inhibited by GDP-mannose in a competitive manner. Furthermore, the activity could be inactivated by 2,3-butanedione suggesting the presence of a catalytic Arg residue. Site-specific mutations at R373, R472, R479, E410, H411, N433 and E458 increase the K_M approximately 8–20-fold. The PMI activity of PslB was completely diminished with a R408K or R408A, reflecting the importance of this residue in catalysis. Overall, these results provide a basis for understanding the catalytic mechanism of PMI.

Keywords: GDP-mannose pyrophosphorylase; *Pseudomonas aeruginosa*; Phosphomannose isomerase; *pslB*; Site-directed mutagenesis

1. Introduction

Phosphomannose isomerase (PMI) catalyzes the reversible interconversion of Fru-6-p and mannose-6-phosphate (Man-6-p) [1]. This reaction links Man-6-p into the mannose metabolism pathway resulting in the generation of GDP-mannose (GDP-Man), an important precursor of many nucleotide sugars such as GDP-rhamnose and GDP-fucose, and for mannosylation of various bacterial structural components such as lipopolysaccharides and glycoproteins [2,3]. PMI also plays an essential role in yeasts and therefore can be regarded as an appropriate target to combat both bacterial and mycotic infections [4].

PMI can be classified into three major types based on sequence similarity and domain organization [5,6]. Type I PMIs are found in all eukaryotes including yeast *Candida albicans*, and certain bacteria including *Escherichia coli*. Type II PMIs are bifunctional enzymes possessing GDP-mannose pyrophosphorylase (GDP-Man PPase)/PMI dual activities and are primarily found in bacteria. Type III PMIs, first identified in *Rhizobium meliloti,* are evolutionally more distinct from the other two PMI types. The structural basis on how these seemingly unrelated proteins can catalyze an identical reaction is not clear.

Pseudomonas aeruginosa PAO1 contains three genes encoding a product homologous with the Type II PMI. These genes, designated *algA*, *wbpW* and *pslB,* are located individually within three distinct polysaccharide biosynthesis gene clusters [3]. AlgA and WbpW have been shown to participate in the production of alginate and A-band lipopolysaccharide, respectively [3,7]. The gene *pslB* is located in a 15-gene *psl* operon required for exopolysaccharide synthesis and biofilm formation [8,9]. Whether PslB is indeed a bifunctional GDP-Man PPase/PMI has not been verified.

The major aim of this study is to address the structural-functional relationship of type II PMIs that is been largely unexplored. We have cloned, overexpressed, and characterized the PMI activity of PslB. This was followed by site-directed mutagenesis of conserved amino acid to identify important residues participating in the PMI activity.

2. Materials and methods

2.1. Overexpression and purification of PslB

E. coli Nova Blue harboring the *pslB* overexpression plasmid was grown in 200 ml Luria–Bertani broth supplemented with 50 μg/ml kanamycin and 100 μ isopropyl thio-β-D-galactopyranoside (IPTG) at 30 °C with vigorous shaking. After 10 h, cells were collected by centrifugation at 3100 rpm for 15 min and washed with 20 mM Tris–HCl, pH 7.5. The pellets were resuspended in 20 mM Tris–HCl buffer and the bacteria disrupted by sonication. Soluble proteins were separated from non-soluble proteins by centrifugation at $14000 \times g$ for 20 min at 4 °C. PslB was purified by nickel-charged affinity chromatography following the standard purification protocol (Novagen). The eluted protein was dialyzed against 20 mM Tris–HCl buffer, pH 7.5, to remove imidazole and the protein concentration was determined by the Bradford method with bovine serum albumin as a standard.

2.2. Determination of the enzyme activity

The PMI activity was determined in a 1-ml reaction mixture containing 50 mM Tris–HCl, pH 7.0, 2 mM $CoCl_2$, 1 mM Man-6-p, 1 mM β-NADP, 5 U phosphoglucose isomerase and 5 U Glc-6-p dehydrogenase. The reduction of β-NADP was measured at 340 nm at 25 °C using a spectrophotometer. The GDP-Man PPase activity was assayed

*Corresponding author. Fax: +886 3 572 9288.
E-mail address: hlpeng@mail.nctu.edu.tw (H.-L. Peng).

Abbreviations: IPTG, isopropyl thio-β-D-galactopyranoside; PMI, phosphomannose isomerase; GDP-Man PPase, GDP-mannose pyrophosphorylase; Man-6-p, mannose-6-phosphate

0014-5793/$34.00
doi:10.1016/j.febslet.2008.09.013

in a reaction mixture containing GDP-Man, 5 mM sodium pyrophosphate, 2 mM $MgCl_2$, 2 mM 3-phosphoglycerate, 20 U glyceraldehyde-3-phosphate dehydrogenase and 10 U phosphoglycerate kinase. The decrease in NADH absorption at 340 nm was monitored by a spectrophotometer [10]. Where indicated, 0.5 mM of Man-1-p, GDP-Man, GTP, UDP-Glc, UDP-Gal, ADP-Glc, TDP-Glc, UDP-GlcN, or sodium pyrophosphate was included in the PMI reaction to determine the inhibition activity of these compounds. For determination of the effects of divalent cation, PslB was dialyzed extensively in 20 mM Tris–HCl, pH 7.5, 140 mM NaCl and 1 mM EDTA. The enzyme activities were determined in the presence of 2 mM chloride form divalent cation including $CaCl_2$, $MnCl_2$, $MgCl_2$, $CoCl_2$, $NiCl_2$ and $ZnCl_2$ [2,11].

2.3. Inactivation of PslB by 2,3-butanedione

PslB (3.2 mg/ml) was incubated with different concentrations of 2,3-butanedione (150 mM borate buffer, pH 9.0) at 22 °C in the dark for 0–60 min [12,13], then the excess 2,3-butanedione was removed by passing the reaction mixture through a Sephadex G-25 column (Pharmacia). The PMI activity was measured as described above.

2.4. Amino acid sequence alignment and site-directed mutagenesis

The multiple sequences alignment of several type II PMIs, including *Xanthomonas campestris* XanB [14], *Helicobacter pyroli* HP0043 [2], *Gluconacetobacter xylinus* AceF [15], and *Vibrio vulnificus* VV0352, were conducted by using the Vector NTI (Invitrogen) and the result is shown in Fig. 5. Site-specific mutations were performed using the QuikChange site-directed mutagenesis kit purchased from Stratagene. Oligonucleotide primer sequences are provided in Supplementary Table S1.

2.5. Circular dichroism spectrum analysis

The CD spectra of wild-type and mutant PslB were recorded by using a CD spectrophotometer (AVIV 62A PS) with 1-mm path length cell, 0.5 nm wavelength step, and an averaging time of 3×10^{-1} s. The protein samples were adjusted to 5 μM before measurement. The CD spectra signals were collected from 190 nm to 260 nm in 20 mM Tris–HCl at 25 °C and averaged over three scans [16].

3. Results and discussion

3.1. PslB possesses PMI and GDP-Man PPase activity

Because the enzymatic activity of PslB has not been reported before, we first examined whether it is indeed a GDP-Man PPase/PMI bifunctional enzyme. Recombinant PslB was purified from *E. coli* by nickel affinity chromatography and its purity confirmed on a SDS–polyacrylamide gel (Fig. 1). Under the standard assay conditions, both GDP-Man PPase and PMI activities could clearly be detected for PslB. The K_M value of Man-6-p for the PMI activity was 1.18 mM, and the K_M of GDP-Man for GDP-Man PPase was 0.11 mM, both values are in good agreement with that reported for AlgA in *P. aeruginosa* 8822 [7]. Bacteria with a large genome commonly harbor duplicated genes encoding functionally identical enzymes. For example, there are at least three UDP-Glc dehydrogenases in *P. aeruginosa* PAO1. The enzyme kinetic parameters and expression profiles are somewhat different for these UDP-Glc dehydrogenases that ensure the bacterium can adapt to broader environments [17]. A similar mode of regulation may also occur for PMI. It has been demonstrated previously that a *P. aeruginosa* strain deficient in WbpW could not produce normal amounts of A-band lipopolysaccharide despite the presence of functional *algA* and *pslB* [3], suggesting that WbpW has distinct expression profiles or kinetic parameters from PslB and AlgA.

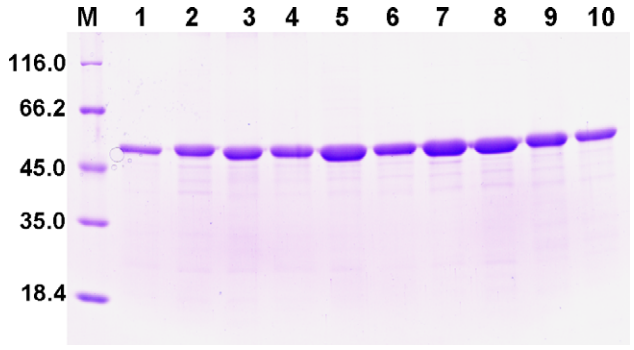

Fig. 1. Protein purity of wild-type and mutant PslB. The samples were resolved on a 0.5% sodium dodecyl sulfate–12.5% polyacrylamide gel. Lanes 1, wild-type; 2, R373A; 3, R408A; 4, R408K; 5, E410A; 6, H411A; 7, N433A; 8, E458A; 9, R472A; 10, R479A.

3.2. Divalent cation requirement for PslB

We measured the PMI and GDP-Man PPase activities of PslB at a fixed concentration (2 mM) of different divalent ions to evaluate cation dependence of the protein. The GDP-Man PPase of PslB could utilize different divalent metal ion with the highest activity in the presence of Mg^{2+}, followed by Co^{2+}, then Mn^{2+} (Table S3). The PMI activity of PslB showed high specificity to Co^{2+}, yielding about 3-fold higher activity than that observed with Mn^{2+} (Table S3). Other divalent cations, including Mg^{2+}, Zn^{2+}, Ca^{2+}, and Ni^{2+}, could not serve

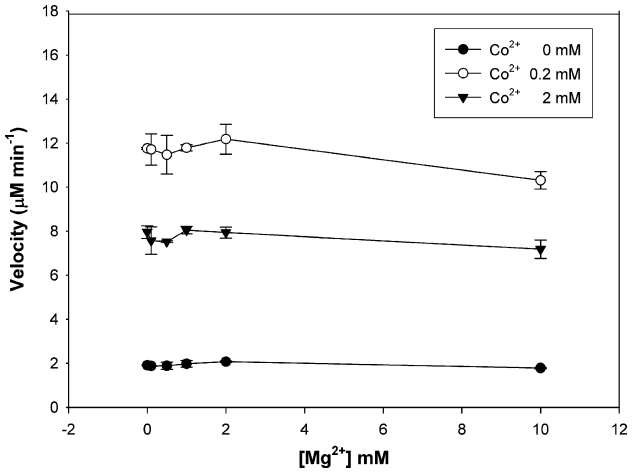

Fig. 2. Effects of Mg^{2+} on the PMI activity of PslB. The assay were performed in the absence (●), and presence of 0.2 mM (○) or 2.0 mM (▼) Co^{2+}.

Table 1
Effects of potential inhibitors on the PMI activity

Potential inhibitor[a]	Relative activity (%)[b]
Control	100 ± 2.2
GTP	106.4 ± 2.4
PPi	120.2 ± 3.5
Man-1-P	77.8 ± 2.5
GDP-Man	46.9 ± 3.9
UDP-GlcN	93.3 ± 3.8
UDP-Gal	105.8 ± 6.9
UDP-Glc	87.4 ± 1.4
ADP-Glc	81.9 ± 3.6
TDP-Glc	78.8 ± 1.2

[a]The PMI activity was analyzed in the presence or absence of 0.5 mM potential inhibitors.
[b]The relative activity was calculated by comparing with control, whose activity was set as 100%.

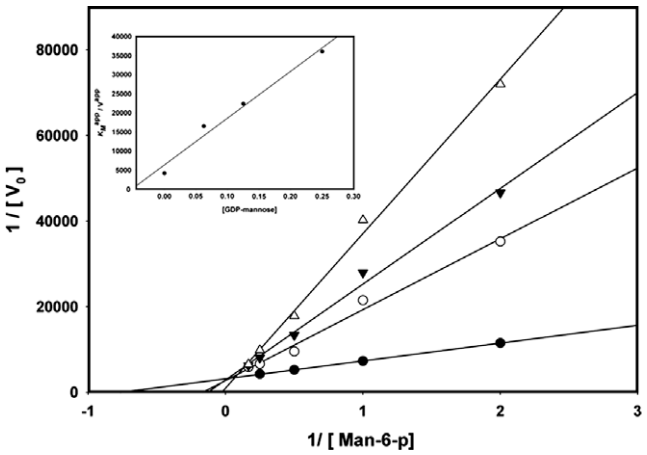

Fig. 3. Double reciprocal plot at various GDP-Man concentrations. The GDP-Man concentrations shown are ●, 0 μM; ○, 62.5 μM; ▼, 125 μM; △, 250 μM. The four lines intersect in the vertical axis representing that they have the same V_{max}. The slopes (slope = K_M/V_{max}) of the lines increase in the present of higher concentration of GDP-Man, indicating that their K_M values increase. Overall, this plot shows a competitive inhibition of GDP-Man for PMI activity. The inset illustrates the reciprocal slopes from Fig. 2 *versus* GDP-Man concentrations.

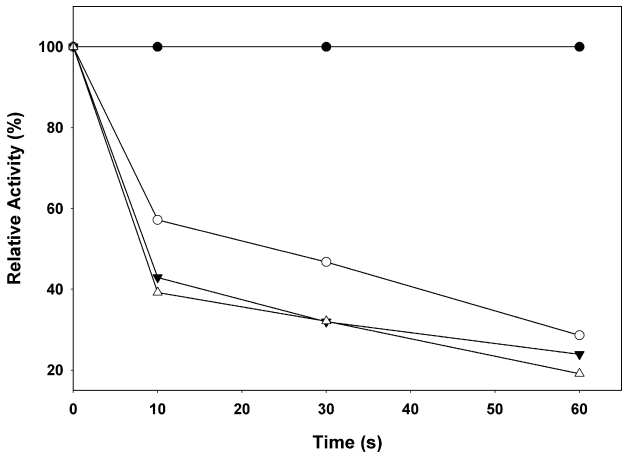

Fig. 4. Inactivation of PslB by 2,3-butanedione. Relative activity (%) was calculated against the activity without 2,3-butanedione. The final concentration of 2,3-butanedione were ●, 0 mM; ○, 20 mM; ▼, 40 mM; △, 80 mM.

effectively as a cofactor for the PMI activity of PslB, consistent with several previous reports [2,7,18]. The optimal Co^{2+} concentration for the PMI was 0.2 mM, which yielded an activity approximately 1.5-fold higher than that of 2.0 mM (Fig. S1). Mg^{2+} at 2.0 mM showed little interference on the PMI activity in the presence of either 0.2 mM or 2.0 mM Co^{2+} (Fig. 2), indicating that Co^{2+} is capable of functioning as a cofactor for the PMI in bacterial cells which commonly contain millimolar Mg^{2+}[19]. Interestingly, both PMI and GDP-Man PPase activities in PslB could not be activated in $ZnCl_2$ despite the fact that the protein contains a zinc-binding sequence $Q^{403}XH^{405}$ (X represents any amino acid), a feature that is also present in type I PMIs [6,7,18].

3.3. The PMI activity of PslB is inhibited by GDP-Man

Several molecules participating in GDP-Man biosynthesis and six nucleotide sugars commonly found in bacteria were tested for their effects on the PMI activity of PslB. At 0.5 mM, only GDP-Man significantly inhibited the PMI activity, which decreased to approximately 47% than that observed for the control (Table 1). Further investigation on the GDP-Man inhibition type demonstrated a competitive inhibition (Fig. 3) indicating that the GDP-Man biosynthesis pathway is well controlled by the end product, GDP-Man, as also is found for *Helicobacter pylori* PMI [2]. A slight deviation of the 250 μM GDP-Man line from the other three lower

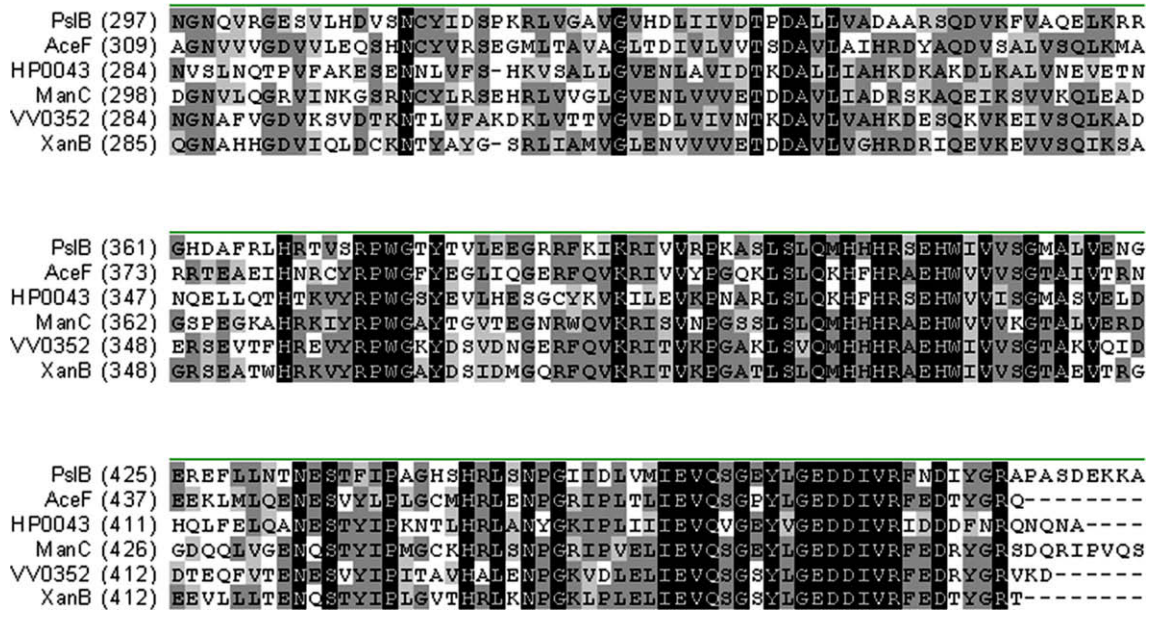

Fig. 5. Amino acid sequence alignment of GDP-Man PPase/PMIs. Only the C-terminal PMI comprising regions of the proteins are shown. The GenBank accession numbers for these proteins are: *Pseudomonas aeruginosa* PslB, AF053957; *Xanthomonas campestris* XanB, B44303; *Helicobacter pyroli* HP0043, AAD056211; *Gluconacetobacter xylinus* AceF, CAA72316; *Vibrio vulnificus* VV0352, NP_933145.

concentration lines was observed suggesting that the inhibition is attenuated in higher concentrations of the inhibitor. The results suggest that the mannose group in GDP-Man competes with Man-6-p at the PMI active site to regulate the mannose utilization in *P. aeruginosa*.

3.4. An Arg residue participates in the P. aeruginosa PMI activity

To identify if PslB is a useful target to combat *P. aeruginosa* infections, it is essential to locate the active site participating in the PMI catalytic activity. It has been shown previously that R304 is an active site residue in a type I PMI of *C. albicans* [20]. Although type I and type II PMI share low amino acid sequence homology, their catalytic mechanisms may be similar. To determine whether an Arg is involved in the PMI activity of PslB, this study utilized 2,3-butanedione to modify Arg in the protein and the PMI activity determined [21]. Fig. 4 shows that the PMI activity decreased with increasing 2,3-butanedione concentrations and the modification time, revealing that at least one Arg residue in PslB is involved in PMI catalysis.

3.5. Arg408 substitutions abolished the PMI activity of PslB

Based on sequence alignment with other type II PMI, R373, R408, R472 and R479 were chosen and changed to an Ala by site-directed mutagenesis. In addition, this study adopted the molecular structure information of *Pyrobaculum aerophilum* bifunctional enzyme phosphoglucose/phosphomannose isomerase (PaPGI/PMI) [22], and selected E410, H411, N433 and E458 for site-directed mutagenesis. The kinetic constants of the wild-type and mutant PslB are shown in Table 2. Substitution of Arg at position 408 to either a Lys or an Ala abolished nearly all of the PMI activity. Other mutant proteins still retained PMI activities and the K_M values were 8–20-fold larger compared to those values observed for wild-type. The CD spectra (Fig. 6) of R408A, R408K and wild-type PslB are nearly identical, all showing a minimum point at 208 nm and 222 nm, a typical spectrum of high α-helix content protein. The data indicate that there is no major alteration of the secondary structures of the mutant proteins.

Overall, the results indicate that R408, which lies within the well-conserved motif shared by most, if not all, type II PMI is an important residue for PMI catalysis. The residue is likely to participate in the interconversion of sugar moieties by providing the binding of the sugar phosphate group or forming the hydrogen bond of sugar hydroxyl group, stabilizing the binding between substrate and enzyme [20].

Table 2
PMI kinetic parameters of the wild-type or mutated PslB

	K_M (Man-6-p, mM)	K_{cat} (s^{-1})[a]	K_{cat}/K_M ($mM^{-1}\ s^{-1}$)
WT	1.18	1.38	1.17
R373A	15.9	0.75	0.05
R408A	ND[b]	ND	ND
R408K	ND	ND	ND
E410A	9.04	2.63	0.29
H411A	16.26	4.41	0.27
N433A	12.92	3.5	0.27
E458A	12.36	3.25	0.26
R472A	23.12	0.25	0.01
R479A	12.28	0.54	0.04

[a] K_{cat} was calculated from the equation $V_{max} = K_{cat} \times [E_o]$, where E_o is the molar concentration of PslB. The results are the average of three independent experiments.
[b] ND, not detected.

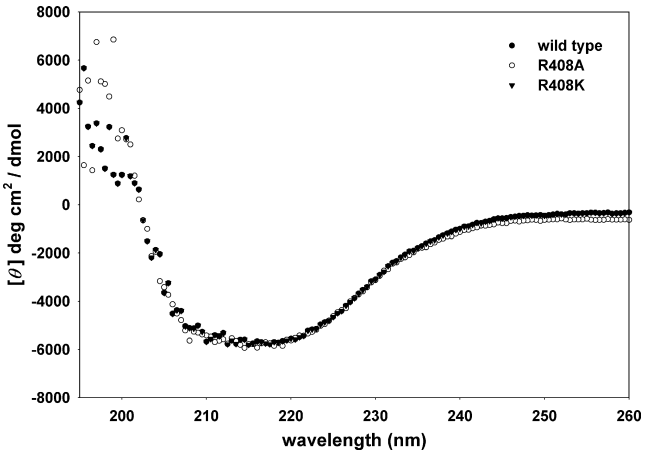

Fig. 6. Circular dichroism spectra of wild-type and mutant PslB. ●, wild-type; ○, R408A; ▼, R408K.

3.6. The R408 mutations did not affect GDP-Man PPase activity of PslB

The fusion of the GDP-Man PPase and PMI domains in the type II PMI implies these two activities may interact with each other. The GDP-Man PPase activity of the PslB deficient in PMI activity was determined and no difference was observed: the K_M values of wild-type, R408A and R408K were 0.068 mM, 0.072 mM and 0.078 mM, respectively. The similar K_M values of wild-type and mutant PslB provide strong evidence that PMI and GDP-Man PPase are actually two independent domains.

Acknowledgement: This work was supported by National Science Council of the Republic of China.

Appendix A. Supplementary data

Supplementary data associated with this article can be found, in the online version, at doi:10.1016/j.febslet.2008.09.013.

References

[1] Cleasby, A. et al. (1996) The X-ray crystal structure of phosphomannose isomerase from *Candida albicans* at 1.7 angstrom resolution. Nat. Struct. Biol. 3, 470–479.
[2] Wu, B., Zhang, Y., Zheng, R., Guo, C. and Wang, P.G. (2002) Bifunctional phosphomannose isomerase/GDP-D-mannose pyrophosphorylase is the point of control for GDP-D-mannose biosynthesis in *Helicobacter pylori*. FEBS Lett. 519, 87–92.
[3] Rocchetta, H.L., Pacan, J.C. and Lam, J.S. (1998) Synthesis of the A-band polysaccharide sugar D-rhamnose requires Rmd and WbpW: identification of multiple AlgA homologues, WbpW and ORF488, in *Pseudomonas aeruginosa*. Mol. Microbiol. 29, 1419–1434.
[4] Proudfoot, A.E., Payton, M.A. and Wells, T.N. (1994) Purification and characterization of fungal and mammalian phosphomannose isomerases. J. Protein Chem. 13, 619–627.
[5] Proudfoot, A.E., Turcatti, G., Wells, T.N., Payton, M.A. and Smith, D.J. (1994) Purification, cDNA cloning and heterologous

expression of human phosphomannose isomerase. Eur. J. Biochem. 219, 415–423.
[6] Jensen, S.O. and Reeves, P.R. (1998) Domain organisation in phosphomannose isomerases (types I and II). Biochim. Biophys. Acta 1382, 5–7.
[7] Shinabarger, D., Berry, A., May, T.B., Rothmel, R., Fialho, A. and Chakrabarty, A.M. (1991) Purification and characterization of phosphomannose isomerase-guanosine diphospho-D-mannose pyrophosphorylase. A bifunctional enzyme in the alginate biosynthetic pathway of *Pseudomonas aeruginosa*. J. Biol. Chem. 266, 2080–2088.
[8] Friedman, L. and Kolter, R. (2004) Two genetic loci produce distinct carbohydrate-rich structural components of the *Pseudomonas aeruginosa* biofilm matrix. J. Bacteriol. 186, 4457–4465.
[9] Jackson, K.D., Starkey, M., Kremer, S., Parsek, M.R. and Wozniak, D.J. (2004) Identification of psl, a locus encoding a potential exopolysaccharide that is essential for *Pseudomonas aeruginosa* PAO1 biofilm formation. J. Bacteriol. 186, 4466–4475.
[10] Duggleby, R.G., Peng, H.L. and Chang, H.Y. (1996) An improved assay for UDPglucose pyrophosphorylase and other enzymes that have nucleotide products. Experientia 52, 568–572.
[11] Sousa, S.A., Moreira, L.M., Wopperer, J., Eberl, L., Sa-Correia, I. and Leitao, J.H. (2007) The *Burkholderia cepacia* bceA gene encodes a protein with phosphomannose isomerase and GDP-D-mannose pyrophosphorylase activities. Biochem. Biophys. Res. Commun. 353, 200–206.
[12] Makinen, K.K., Makinen, P.L., Wilkes, S.H., Bayliss, M.E. and Prescott, J.M. (1982) Photochemical inactivation of Aeromonas aminopeptidase by 2,3-butanedione. J. Biol. Chem. 257, 1765–1772.
[13] Walker, J.M. (2002) The Protein Protocols Handbook, Humana Press, Totowa, N.J., pp. 475–476.
[14] Koplin, R., Arnold, W., Hotte, B., Simon, R., Wang, G. and Puhler, A. (1992) Genetics of xanthan production in *Xanthomonas campestris*: the xanA and xanB genes are involved in UDP-glucose and GDP-mannose biosynthesis. J. Bacteriol. 174, 191–199.
[15] Griffin, A.M., Poelwijk, E.S., Morris, V.J. and Gasson, M.J. (1997) Cloning of the aceF gene encoding the phosphomannose isomerase and GDP-mannose pyrophosphorylase activities involved in acetan biosynthesis in *Acetobacter xylinum*. FEMS Microbiol. Lett. 154, 389–396.
[16] Coligan, J.E. (2003) Current Protocols in Protein Science, John Wiley & Sons Inc., Brooklyn, NY, Unit 7.6.
[17] Hung, R.J., Chien, H.S., Lin, R.Z., Lin, C.T., Vatsyayan, J., Peng, H.L. and Chang, H.Y. (2007) Comparative analysis of two UDP-glucose dehydrogenases in *Pseudomonas aeruginosa* PAO1. J. Biol. Chem. 282, 17738–17748.
[18] Papoutsopoulou, S.V. and Kyriakidis, D.A. (1997) Phosphomannose isomerase of *Xanthomonas campestris*: a zinc activated enzyme. Mol. Cell Biochem. 177, 183–191.
[19] Hurwitz, C. and Rosano, C.L. (1967) The intracellular concentration of bound and unbound magnesium ions in *Escherichia coli*. J. Biol. Chem. 242, 3719–3722.
[20] Wells, T.N., Scully, P. and Magnenat, E. (1994) Arginine 304 is an active site residue in phosphomannose isomerase from *Candida albicans*. Biochemistry 33, 5777–5782.
[21] Rogers, T.B., Borresen, T. and Feeney, R.E. (1978) Chemical modification of the arginines in transferrins. Biochemistry 17, 1105–1109.
[22] Swan, M.K., Hansen, T., Schonheit, P. and Davies, C. (2004) Structural basis for phosphomannose isomerase activity in phosphoglucose isomerase from *Pyrobaculum aerophilum*: a subtle difference between distantly related enzymes. Biochemistry 43, 14088–14095.